Journal of Molecular Liquids 220 (2016) 101–107

Contents lists available at ScienceDirect

Journal of Molecular Liquids

journal homepage: www.elsevier.com/locate/molliq

Synthesis and properties of two surfactants containing polyoxypropylene block and short branched alkyl chain

Wanxu Wang, Jianbo Li, Xiaoyi Yang *, Ping Li *, Chaohua Guo, Quanhong Li

China Research Institute of Daily Chemical Industry, Taiyuan, Shanxi 030001, PR China

ARTICLE INFO

Article history:
Received 2 February 2016
Received in revised form 5 April 2016
Accepted 11 April 2016
Available online xxxx

Keywords:
Branched tail
Propoxylation
Krafft point
Surface properties
Salt tolerance

ABSTRACT

Short branched alkyl polyoxypropylene sulfates, sodium isohexyl polyoxypropylene sulfate (i-HPS) and sodium isooctyl polyoxypropylene sulfate (i-OPS) were synthetized via propoxylation, sulfation, and neutralization three-step reactions, and characterized by FT-IR and ^{1}H NMR. Their Krafft points were measured and the results were all below freezing point. Their critical micelle concentrations (cmc) and minimum surface tension (γ_{cmc}) determined by equilibrium surface tension were 54.74 mmol L^{-1} and 32.12 mN m^{-1} for i-HPS, 15.57 mmol L^{-1} and 33.33 mN m^{-1} for i-OPS, respectively. The measurement of dynamic surface tension indicated that both the equilibrium values of surface tension and the time required for reaching the equilibrium decreased with the increasing concentration of surfactant solutions. The spreading ability on paraffin film researched through dynamic contact angle revealed that the droplet of i-HPS solution presented a minimum contact angle of 58.9° at a concentration of 150 mmol L^{-1}, while the equilibrium contact angle of i-OPS droplet was 52.8° under the same condition. Their salt tolerance measurement showed that 1.0 wt% i-HPS solution and 1.0 wt% i-OPS solution could endure 183.1 g L^{-1}, 143.9 g L^{-1} NaCl, 206.3 g L^{-1}, 198.4 g L^{-1} $MgCl_2$, and 229.7 g L^{-1}, 217.9 g L^{-1} $CaCl_2$, respectively.

1. Introduction

Alkyl polyoxypropylene sulfates (APS), one kind of extended surfactants, consist of hydrophobic alkyl chain, hydrophilic sulfate group, and poly(propylene oxide) linker as intermediate polarity group to provide a smooth transition between the hydrophobic and hydrophilic parts [1,2]. The insertion of propylene oxide (PO) into hydrophilic head and hydrocarbon tail contributes to the surfactant not only extending its tail length without sacrificing its own water solubility but also acting as one component of the middle phase microemulsions which possess superior solubilization capacity and ultralow interfacial tension (IFT) [2–4]. The APS with such unique surfactant molecular structure have been widely studied due to their extensive applications in soil and aquifer remediation, enhanced oil recovery, pharmaceutical formulations, nanoparticle preparations and froth flotation [5–7].

Phan T.T. et al. [8] researched the effect of structure of APS, which involves the number of PO units and the branching of hydrophobic chain, on the microemulsion formation and IFT values. They found that both the optimum salinity and minimum IFT values decreased with the increase of the inserted PO units or the degree of branching of the hydrocarbon tail. Angelika K. et al. [2] studied the effects of a series of anions and cations on the cloud point of a long hydrophobic chain extended surfactant through phase behavior observation and micelle structure investigation. Their experiments showed that the changes of the surfactant solubility caused by the addition of salts followed the same order as Hofmeister series. Zeng J.X. et al. [9] synthetized a series of APS with different PO adduct numbers through Williamson reaction, sulfating with chlorosulfonic acid and neutralizing with sodium hydroxide. They determined the structure of synthesized compounds and found out that APS could decrease the IFT between aqueous solution and model oil to a low value.

The APS reported in the literatures above have shown excellent performances in microemulsion, IFT, and salt tolerance. However, the sulfating agents used in the synthesis of APS cause a massive amount of waste acid and other pollutants during the sulfonation reaction, which lead to an increase in energy consumption further. Therefore, it is of great importance to develop an environmental friendly and economical sulfating method occupying vapor SO_3. However, to the best of our knowledge, the related research has not yet been reported. In addition, the performances of APS were focused on their functions combined with other components, while the physical and chemical properties of single APS aqueous solution have not been investigated systematically. Hence, an economical and practical sulfating method for synthetizing APS is a pioneer of APS industrialization. The APS fundamental research can expand its application to various fields such as coating technology, mineral flotation and other surface science technology.

In this article, two APS with branching hydrophobic chain, sodium isohexyl polyoxypropylene sulfate (i-HPS) and sodium isooctyl

* Corresponding authors at: China Research Institute of Daily Chemical Industry, 34 Wenyuan Street, Taiyuan, Shanxi Province 030001, PR China.
E-mail addresses: yxywlyzx@163.com (X. Yang), yipingli_@126.com (P. Li).

http://dx.doi.org/10.1016/j.molliq.2016.04.034
0167-7322/

polyoxypropylene sulfate (i-OPS) were synthesized through sulfating with vapor SO_3. Their structures were confirmed by FT-IR and ^1H NMR. Sodium isooctyl polyoxyethylene sulfate (i-OES) and sodium hexyl polyoxypropylene sulfate (HPS) were also synthesized through the same method for comparing with i-OPS and i-HPS to show how the differences between ethylene oxide (EO) groups and PO units, branched chain and straight tail would impact on the Krafft point, minimum surface tension (γ_{cmc}), and critical micelle concentration (cmc). Moreover, dynamic surface tension, dynamic contact angle and salt tolerance of i-HPS and i-OPS aqueous solutions were measured by bubble pressure method, sessile drop technique, and ultraviolet-visible detector, respectively.

2. Experimental methods

2.1. Materials

Isooctyl alcohol (99%), *n*-octanol (98%), *n*-hexyl alcohol (98%), absolute ethanol (99.7%), cyclohexane (98%), sodium chloride (NaCl 99.6%), magnesium chloride ($MgCl_2$ 98%), and calcium chloride ($CaCl_2$ 96%) were supplied by Tianjin Kermel Chemical reagent Co., Ltd. (China) and used without further purification. Acetone (98%), sodium hydroxide (96%), and fuming sulfuric acid (65% concentration) were purchased from Tianjin Shentai Chemical reagent Co., Ltd. (China). Isohexyl alcohol (98%) was provided by TCI Development Co., Ltd. (Shanghai). PO (99.5%) was offered by Sinopharm Chemical reagent Co., Led. (China). The catalyst was prepared by our workgroup in advance. The deionized water with a resistivity of 18.25 MΩ·cm prepared by a UPD-II ultrapure water purifier was used in the preparation of all solutions.

2.2. Synthesis and characterization

2.2.1. Synthesis of i-HPS and i-OPS

Two surfactants, i-HPS and i-OPS were synthesized by a three-step reaction as shown in Scheme 1.

The autoclave charged with isohexyl alcohol (102.17 g) or isooctyl alcohol (130.23 g) and catalyst (0.70 g) was pumped and filled with nitrogen three times to remove oxygen under stirring and heating. Then, PO (6 g) was put into the reactor to induce the reaction at a temperature of 150 °C. When the system was heated to 165 °C by the energy of chemical reaction, a required amount of PO (169 g) was gradually added into the reactor under a stable pressure of 0.30 MPa. Finally, the mixture was separated using filtration after aging and cooling. Thus, the intermediate product with an average of 3 PO units, isohexyl polyoxypropylene ether alcohol (i-HP) or isooctyl polyoxypropylene ether alcohol (i-OP), was obtained.

The target products, i-HPS and i-OPS, were sulfated, neutralized and purified by the method described in our previous article [10]. The dried surfactants, a light yellow wax-like solid at room temperature, cannot crystallize owing to the polydispersity of the PO units [1].

2.2.2. Structural characterization

The intermediate products (i-HP, i-OP) and target products (i-HPS, i-OPS) were dissolved in respective absolute ethanol and each of the solutions was smearing onto KBr prisms. Then, FT-IR for the products was recorded via a Bruker Vertex-70 spectrometer, respectively. ^1H NMR spectra for the target product $CDCl_3$ solutions was detected on a Varian INOVA-400 Hz spectrometer, respectively.

2.3. Krafft point

The method for determining the Krafft points of experimental products and control products was described in literatures [10,11]. The solutions with a concentration of 1.0 wt% were cooled to cloudy after the process of using ultrasonic technique to form a homogeneous continuous phase. Then, the heterogeneous solutions were heated gradually to clear again under a heating rate of 0.5 °C min^{-1}. The temperature at which the system became clear was the Krafft point of surfactant. For each measurement, the reported Krafft point was the average value of three replications.

2.4. Equilibrium surface tension

The surface tension (γ) was obtained by a Krüss K12 Processor Tensiometer (Krüss Company, Germany, accuracy ± 0.01 mN m^{-1}) via the Wilhelmy plate method at 25 ± 0.1 °C. The recorded value of each concentration was the mean value determined from the three repeated measurements with an interval of 30 s. The γ of ultrapure water (72.0 ± 0.3 mN m^{-1}) was carried out before the measurement to make sure that the silica dish had no impurity.

2.5. Dynamic surface tension

Dynamic surface tension was conducted on a Krüss BP-100 bubble pressure tensiometer (Krüss Company, Germany, accuracy ± 0.01 mN m^{-1}) with a range of effective surface ages from 10 to 200,000 ms at 25 ± 0.1 °C. Ultrapure water was used for calculating the internal diameter of capillary in advance.

2.6. Dynamic contact angle

Dynamic contact angle was measured using a drop shape analyzer DSA-25 (Krüss Company, Germany, accuracy ±0.1°) to judge the spreading property of the target product aqueous solution on paraffin film at 25 ± 0.1 °C. The ultrapure water drop with a contact angle of (106 ± 2)° on paraffin substrate [12] was performed before measuring to ensure the system was clean. The final value of each sample was the average data from three droplets recorded at an air humidity of (55 ± 5)%.

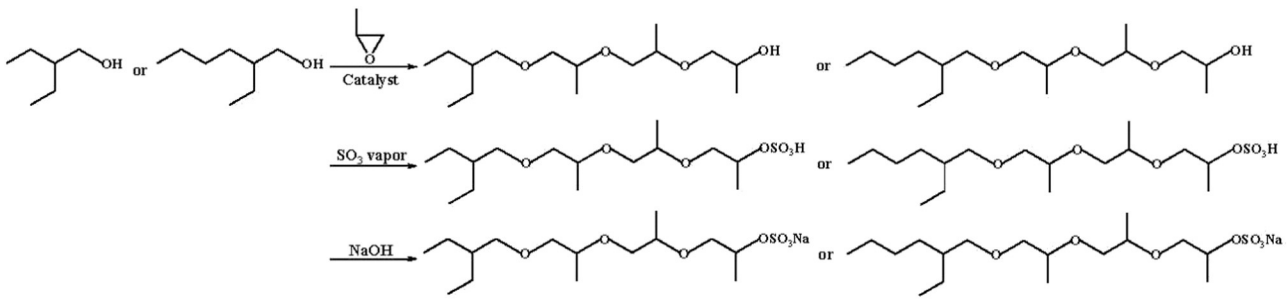

Scheme 1. Synthetic routes of i-HPS and i-OPS.

2.7. Salt tolerance

The transmittance of the 1.0 wt% surfactant aqueous solutions containing different amount of salt at 600 nm was carried out via a UV-1601 UV/VIS spectrophotometer (Beijing Rayleigh Analytical Instrument Co., Ltd, China, photometric accuracy ±0.3%T) at 15 ± 2 °C to investigate the salt tolerance of the target products. The salts involving the measurements include NaCl, $CaCl_2$, and $MgCl_2$. The solutions with different content of salt were stirred before the measurement.

3. Results and discussion

3.1. Structure of the products

Fig. 1 is the FT-IR spectra of the intermediate products and target products. We emphatically analyze the information shown in Fig. 1 (A) in which reveals the FT-IR of i-HP (a) and i-HPS (b). The strong absorption peak of hydroxyl stretching region at 3400 cm^{-1} in Fig. 1(A-a) is weaken significantly in Fig. 1 (A-b) through sulfating reaction. And meanwhile, the intense symmetric stretching vibration peak of sulfur-oxygen double bond at 1245 cm^{-1} and the broad stretching vibration peak of C–O–S at 770 cm^{-1} appear in Fig. 1 (A-b). The appearance of these two phenomena at the same time indicates that the hydroxyl has been substituted by sulfate group [9]. In addition, the weak peak of hydroxyl in Fig. 1 (A-b) could be caused by the sample smeared on the KBr plate with a residue of ethanol [10].

The ^{1}H NMR spectra of the target products are shown Fig. 2, in which a number of information revealed in the two spectra overlaps seriously owing to the surfactants belong to a homologous series. As a result of the polydispersity of polypropylene segments in the products, the chemical shifts of hydrogen atoms in molecules are superposed in the spectra, which would lead to the indistinction of the splitting peaks. While the number of hydrogen atom of each group can be calculated by the integrate areas of respective proton peaks. The assignment and corresponding number of hydrogen atom of peaks in Fig. 2 are listed below, respectively.

For i-HPS in Fig. 2 (A), δ: 0.835 (6H, –CH_3 of the isohexyl), 1.131 (4H, –CH_2–), 1.306 (9H, –CH_3 of the PO groups), 1.427 (1H, methylidyne of the hydrophobic chain), 3.312 (2H, –CH_2–O), 3.493 (6H, O–CH_2–methylidyne), 3.916 (2H, O–CH_2–), 4.696 (1H, methylidyne of the PO unit closest to the sulfate group), 7.260 ($CDCl_3$).

For i-OPS in Fig. 2 (B), δ: 0.871 (6H, –CH_3 of the tail), 1.142 (8H, –CH_2–), 1.241 (9H, –CH_3 of the PO units), 1.489 (1H, methylidyne of the isooctyl), 3.331 (2H, –CH_2–O), 3.533 (6H, O–CH_2–methylidyne), 3.904 (2H, O–CH_2–), 4.719 (1H, methylidyne of the PO group nearest the sulfate group), 7.260 ($CDCl_3$).

The results of structure characterization show that the target surfactants, i-HPS and i-OPS, are synthesized successfully.

3.2. Krafft point

Krafft point is a specific temperature at which the ionic surfactant aqueous solution presents an equilibrium among micelles, monomers, and undissolved surfactant at a certain pressure. In other words, Krafft point is the temperature where the solubility of ionic surfactant equals to its cmc at a given pressure. The solubility will have a rapid augmentation and the micelles are formed in a large amount when the temperature of solution slightly exceeds its Krafft point [13,14]. The temperature involving such useful properties exerts an increasing important effect on foam flotation and metal cleaning at low temperature. In general, the Krafft point of surfactant will be viewed as below 0 °C if its 1.0 wt% solution still remain clarify when ice and water coexist. The Krafft points of i-OPS, i-OES, i-HPS, and HPS are listed in Table 1 and all below freezing point.

The introduction of short hydrophobic chain or branched tail to the target products can reduce the intermolecular force between the surfactant molecules in solid state [15]. The PO units extend the effective length of carbon chain to a certain degree, but they do not sacrifice the solubility of surfactant and instead introduce the branching to weaken the interaction of surfactant. For i-OES, the reasons lead to its low Krafft point have been discussed in our previous literature [10]. The surfactant with low Krafft point means that it has a high solubility at low temperature, which can extend its actual application under different environment conditions.

3.3. Equilibrium surface tension

The surface activity of i-OPS, i-OES, i-HPS, and HPS is evaluated by the equilibrium surface tension. In Fig. 3, the γ of the four surfactants aqueous solutions gradually decrease with the increase of their concentrations and finally reach respective plateaus at 25 °C, indicating that the amphiphilic molecules diffuse to the air/liquid interface and then attain saturation on the interface [16]. The curves of γ show two inflection points versus the logarithm of the concentrations of surfactants solutions. The appearance of the first inflection point may be caused by the formation of the premicellar aggregates [17,18]. The cmc and corresponding γ_{cmc} are obtained by the intersection point of fitting straight lines of the second decreasing stage and the plateau portion. The saturation adsorption values (Γ_{max}) and the minimum area occupied by a single amphiphilic molecule (A_{min}) at the air/liquid interface are derived by the Gibbs adsorption isotherm equations [16,18] (Eqs. (1) and (2)). The parameter, pC_{20} advanced by Rosen et al. [19], is computed by the

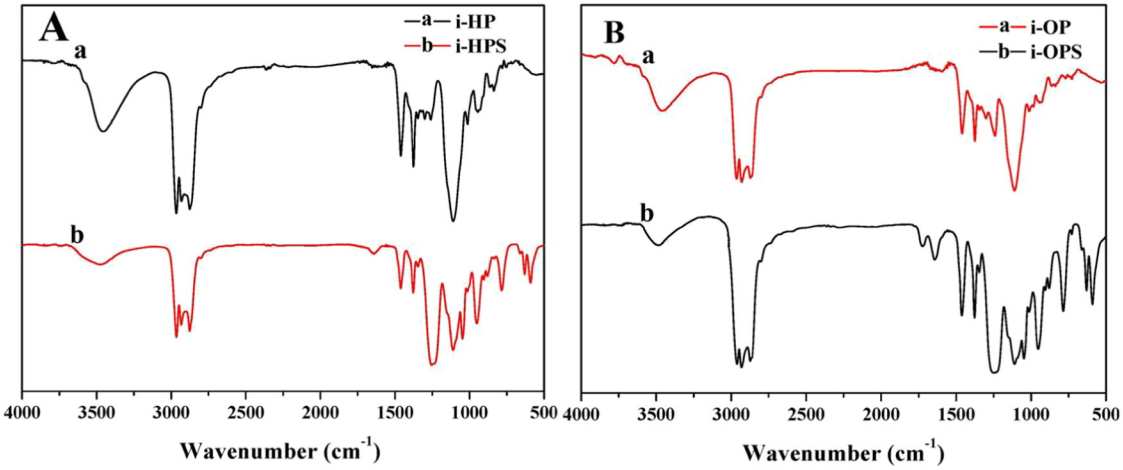

Fig. 1. FR-IR spectra of i-HP (A-a), i-HPS (A-b), i-OP (B-a), and i-OPS (B-b).

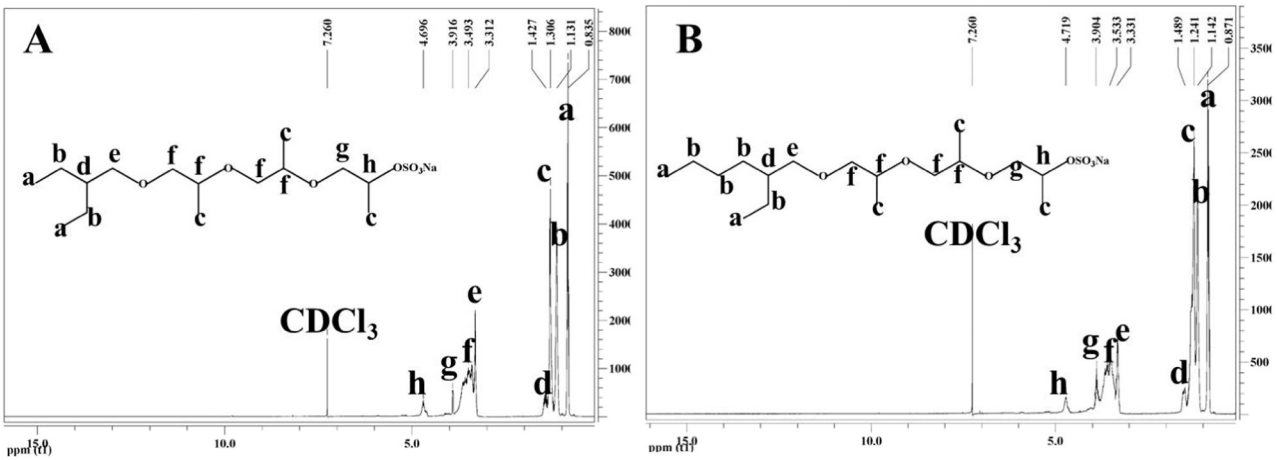

Fig. 2. ^{1}H NMR spectra of i-HPS (A) and i-OPS (B).

negative logarithm of surfactant concentration at which the surface tension of solution has a 20 mN m^{-1} reduction compared with that of pure solvent (Eq. (3)) to denote the adsorption efficiency of surfactant. The large pC_{20} implies that the amphiphilic molecules can adsorb at the air/liquid interface easily and the γ of solution can be reduced at low concentration of surfactant. Their numerical values are listed in Table 1.

$$\Gamma_{max} = -(\partial\gamma/\partial 1\ g\ C)_T/2.303nRT \quad (1)$$

$$A_{min} = 10^{16}/N_A\Gamma_{max} \quad (2)$$

$$pC_{20} = -1\ g\ C_{20} \quad (3)$$

Where R, T, N_A, n, and $\partial\gamma/\partial lgC$ represent the gas constant (8.314 J mol^{-1} K^{-1}), absolute temperature, Avogadro's constant, Gibbs prefactor related to the species of surfactant adsorbed at the interface (for ionic surfactant, $n = 2$), and the slope of the premicellar region in the curve of γ against log concentration.

From Table 1, we can see that the cmc of i-OPS and i-OES are 15.57 mmol L^{-1} and 21.67 mmol L^{-1}. They are smaller compared to those of HPS and i-HPS which are 50.59 mmol L^{-1} and 54.74 mmol L^{-1} because the chain length of isooctyl is longer than that of isohexyl and the hydrophobicity of isooctyl is higher than hexyl's [20]. Compared with EO groups, the PO units with intermediate polarity, in a manner, extend the length of hydrophobic chain which makes the cmc of i-OPS lower than i-OES's. Owing to the reduction of the effective length of hydrocarbon chain by the introduction of branching, the cmc of i-HPS is greater than that of HPS which has leaner tail and equal carbon number compared to i-HPS. The γ_{cmc} of branched surfactants are lower than that of straight surfactant as a result of the increasing of effective hydrocarbon density at the air/liquid interface contributed by the more hydrophobic branching structure [21]. The γ_{cmc} of i-OES is lower compared to other surfactants, which may be caused by the increasing dispersion of the surfactant molecular arrangement through embedding EO repeat units and expanding the area of hydrophilic group. It is observed that the A_{min} is sorted from big to small: i-OPS, HPS, i-HPS, and i-OES. The flexible PO units structure near the head group, the length of hydrophobic chain and the presence of branching in the hydrophobic chain may all attribute to the ranked and explain the Γ_{max} order of the four surfactants.

Table 1
Krafft points and adsorption parameters for HPS, i-HPS, i-OPS, and i-OES aqueous solutions at 25 °C.

Surfactants	Krafft point	cmc	γ_{cmc}	Γ_{max}	A_{min}	pC_{20}
	°C	mmol L^{-1}	mN m^{-1}	mmol m^{-2}	Å^2	
HPS	<0	50.59	33.47	0.23	722.2	2.7
i-HPS	<0	54.74	32.12	0.24	692.1	3.1
i-OPS	<0	15.57	33.33	0.21	808.7	3.3
i-OES	<0	21.67	27.40	0.39	422.9	3.5

3.4. Dynamic surface tension

The adsorption kinetics of surfactant at the air/liquid interface is commonly studied through the dynamic surface tension data from the maximal bubble pressure technique [22]. The curves of dynamic surface tension against the surface age for surfactant aqueous solutions with different concentrations are shown in Fig. 4. It can be noticed that both the reducing extent and the reducing rate of the surface tension increase remarkably with the concentration of surfactant solution increasing. The time needed to reach the absorption equilibrium, meanwhile, is drastically shortened. In addition, the dynamic surface tensions of i-HPS in Fig. 4 (A) are higher than these of i-OPS in Fig. 4 (B) with the same concentrations, which has the same trend compared to the equilibrium surface tension of i-HPS and i-OPS, indicating that i-OPS molecules prefer to adsorb at the air/liquid interface. The reason caused the dynamic behavior may be the interaction between hydrophobicity of the branched tail and molecular weight under the premise of presenting the same hydrophilic content and PO units [23]. The strong hydrophobicity contributes to the molecules escape from the bulk phase to the air/liquid interface, while the high molecular weight slows down the diffusion of surfactant molecules. In this case, the promoting effect of

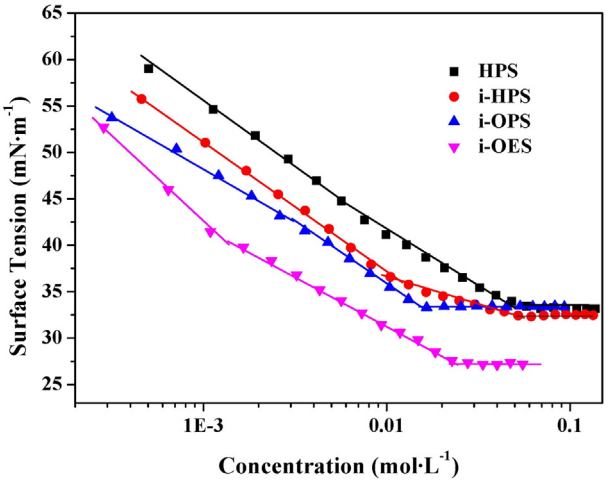

Fig. 3. Surface tensions of HPS, i-HPS, i-OPS, and i-OES aqueous solutions against their log molar concentrations at 25 °C.

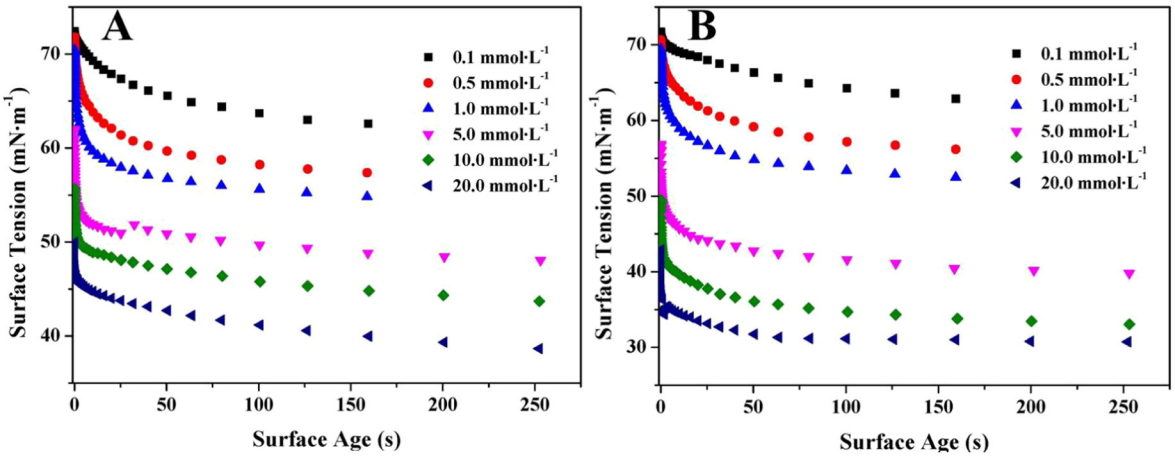

Fig. 4. Dynamic surface tensions of i-HPS (A) and i-OPS (B) aqueous solutions with different concentrations at 25 °C as a function of surface age.

hydrophobicity may have an edge compared to the impeditive function of molecular weight in the diffusion process for i-HPS and i-OPS.

3.5. Dynamic contact angle

In the practical applications, such as washing and mineral flotation, the surfactant is needed to help the solvent wet the oil/water or solid/liquid interface. The spreading ability is a fundamental and applied property of surfactant solution between two phases. The spreading performance of i-HPS and i-OPS solutions on the substrate is investigated through the most useful dynamic contact angle measurement, which determines the angles between the air/liquid interface and the solid/liquid interface with a common solid/liquid spot [24]. The contact angles of droplets with different surfactant concentrations on the parafilm versus the time are shown in Fig. 5, respectively. As can be seen from Fig. 5, the contact angles of droplets decrease rapidly and reach lower equilibrium values with the increase of the concentration of surfactants. Both the starting and equilibrium contact angles of i-HPS in Fig. 5 (A) are larger than those of i-OPS in Figure5 (B), which responds the phenomenon of dynamic surface tension mentioned above.

The low contact angle involving the molecular orientation is decided by the low γ of the droplet attributed to the branched tail structure of the surfactant molecule. The molecules with stronger hydrophobic chain are more eager to transfer from solution to the solid/liquid interface, which is the hydrophobic effect driven by entropy [25]. The introduction of branching and PO units makes a contribution to the formation of closely packed monolayer which presents the structure with hydrophobic chain pointed outward of the droplet while the head group extended into water phase. The outer layer of the droplet is similar to the alkane film with an excellent wetting ability on substrate with low energy when the adsorption of surfactant approaches saturation [26]. Thus, the essential of wetting ability of solution on solid surface is the interaction between of solid surface and hydrophobic region of surfactant. The difference between the contact angles of i-OPS and i-HPS in Fig. 5 may be caused by the different tightness of hydrocarbon chain on the surface adsorption layer. The tighter the molecules arrange, the better the wetting ability is.

3.6. Salt tolerance

The presence of moderate salt in surfactant solution can improve the interfacial activity, affect the aggregation behavior of molecules at interface or in bulk phase, and change the partitioning coefficient of surfactant in oil and in water [27]. However, excess salt in solution will lead to precipitation of surfactant and cloudy solution, which finally invites the reduction of related surfactant activities. The maximum salt tolerance of surfactant is a significant critical value to grasp the supplemental dosage of salt for maximal surfactant activities. In addition, the critical concentration of salt at which lead to surfactant precipitate is enslaved to the structure, composition, and concentration of surfactant, regulated by the species and valence of the counter ion, and temperature of the solution. Fig. 6 (A) and (B) show that the transmittance of solutions with 1.0 wt% surfactant at 600 nm against the amount of salt added at 15 ± 2 °C. The specific tolerance values of i-HPS and i-OPS to NaCl, $MgCl_2$,

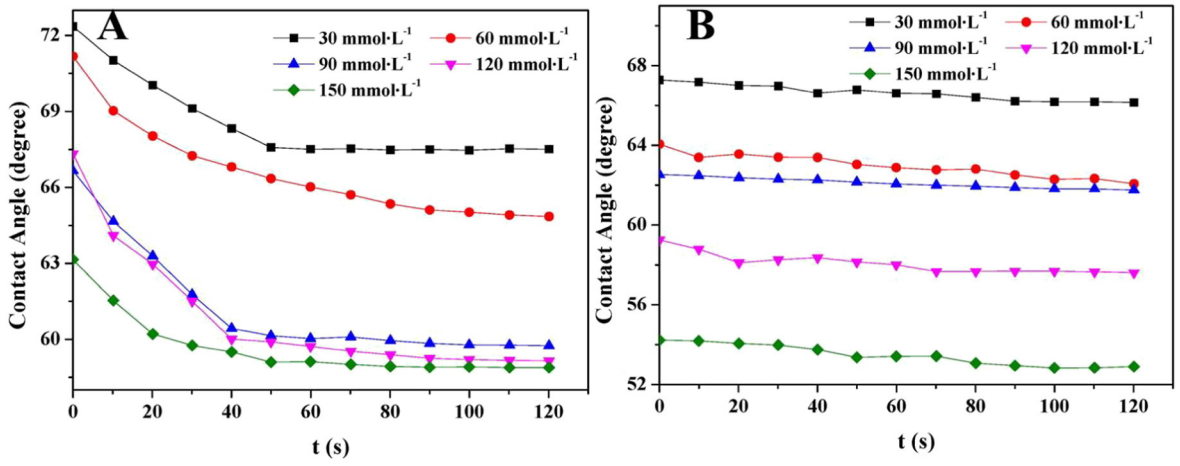

Fig. 5. Contact angles with time for droplets of i-HPS (A) and i-OPS (B) aqueous solutions with different concentrations at 25 °C.

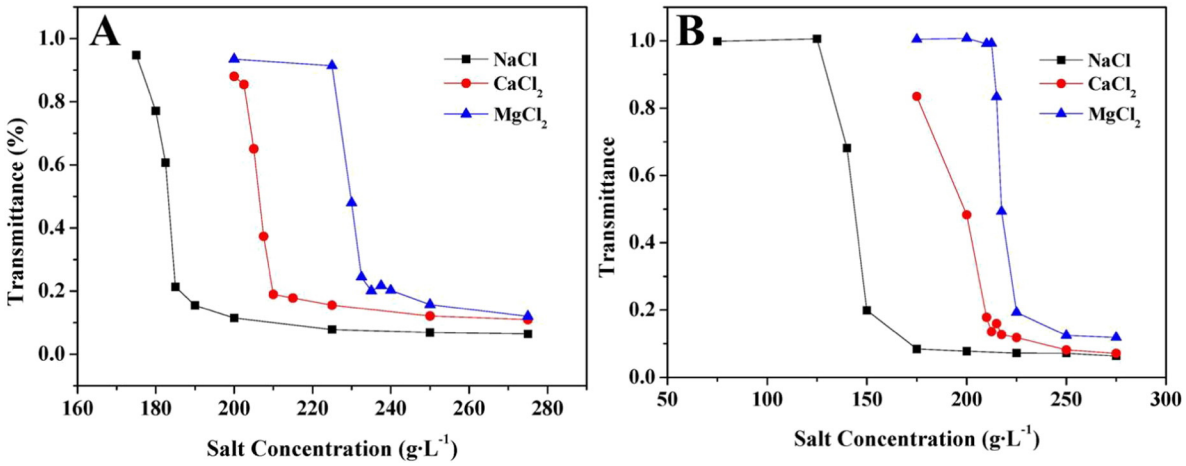

Fig. 6. Transmittance versus electrolyte concentration for i-HPS (A) and i-OPS (B) aqueous solutions with a concentration of 1.0 wt% at 15 °C.

and $CaCl_2$ in aqueous solution are listed in Table 2 when the transmittance is 0.5. From it, we can see that the salt tolerance of i-OPS is lower than that of i-HPS.

Generally, when the aggregations form in the solution with a concentration above cmc, the salt will effect the aggregation behaviors of ionic surfactant remarkably [27]. Such as at high salt concentration, the aggregations are asymmetric micelles which will impact the rheological behavior and stability of the solution [28]. The hydrated layer of head group of surfactant molecule and the electrical double layer of micelle are compressed due to the strong electrostatic interaction among counter ions, surfactant ions, and micelles, which leads to the areas of head groups of surfactant in micelles decrease and the sizes of micelles increase sharply. Several cations can be adsorbed at the surrounding of one head group of surfactant because of the small size of inorganic ions. The adsorption state may reduce the net charge of micelles so that increase the size of micelles and decrease the surface charging amount. Such changes may result in the reduction of electrostatic repulsion between micelles and the formation of larger aggregations. Furthermore, the solution may become turbid and present phase separation. While for sulfate surfactants, the two p-d π dative bonds between sulfur and oxygen of –SO_3H group strengthen the electron withdrawing ability of sulfur from hydroxyl, which makes hydroxyl dissociate easily and free energy reduce. The stable –SO_3^- has a weak attraction for cations, which hampers cations enter the hydrated layer of –SO_3^- easily. Thus, i-OPS and i-HPS present excellent Na^+, Mg^{2+}, Ca^{2+} tolerance.

4. Conclusions

Two novel short branched alkyl polyoxypropylene sulfates surfactants were successfully synthesized by the alkoxylation of branched alcohol and the sulfation using SO_3 gas. Their structures were determined by FT-IR and ^1H NMR. Their physicochemical properties were investigated through a series of measurements. The results showed that both the Krafft points of i-HPS and i-OPS were below 0 °C, the cmc and γ_{cmc} of i-HPS were 54.74 mmol L^{-1} and 32.12 mN m^{-1}, the cmc and γ_{cmc} of i-OPS were 15.57 mmol L^{-1} and 33.33 mN m^{-1}, respectively.

Table 2
Tolerance values of i-HPS and i-OPS to NaCl, $MgCl_2$, and $CaCl_2$ in aqueous solution when the transmittance is 0.5 at 15 °C.

Surfactant	NaCl	$MgCl_2$	$CaCl_2$
	g L^{-1}	g L^{-1}	g L^{-1}
i-HPS	183.1	206.3	229.7
i-OPS	143.9	198.4	217.9

In addition, the dynamic surface tension data revealed that i-OPS molecules were more disposed to adsorb at the air/liquid interface than i-HPS molecules. Likewise, the measurement of dynamic contact angle on paraffin film indicated that i-OPS molecules were more eager to transfer from solution to the solid/liquid interface than i-HPS molecules. These meant that surfactant molecules with stronger hydrophobic chain would like to escape from the bulk phase to the hydrophobic interface. However, the study on salt tolerance signified that i-HPS possessed an excellent stability of salt tolerance compared to i-OPS. Hence, the introduction of branched tail and PO units to surfactant molecule can impact on the adsorption and aggregation behaviors of surfactant, which will play a significant role in agriculture adjuvant, mineral flotation, and other surface-related science.

Acknowledgements

This project is funded by the Shanxi Province Science Foundation for Youths (No. 2015021052).

References

[1] A. Klaus, G.J.T. Tiddy, C. Solans, A. Harrar, D. Touraud, W. Kunz, Effect of salts on the phase behavior and the stability of nano-emulsions with rapeseed oil and an extended surfactant, Langmuir 28 (2012) 8318–8328.
[2] A. Klaus, G.J.T. Tiddy, R. Rachel, A.P. Trinh, E. Maurer, D. Touraud, W. Kunz, Hydrotrope-induced inversion of salt effects on the cloud point of an extended surfactant, Langmuir 27 (2011) 4403–4411.
[3] A. Witthayapanyanon, T.T. Phan, T.C. Heitmann, J.H. Harwell, D.A. Sabatini, Interfacial properties of extended-surfactant-based microemulsions and related macroemulsions, J. Surfact. Deterg. 13 (2010) 127–134.
[4] A. Witthayapanyanon, E.J. Acosta, J.H. Harwell, D.A. Sabatini, Formulation of ultralow interfacial tension systems using extended surfactants, J. Surfact. Deterg. 9 (2006) 331–339.
[5] D.A. Sabatini, R.C. Knox, J.H. Harwell, B. Wu, Integrated design of surfactant enhanced DNAPL remediation: efficient supersolubilization and gradient systems, J. Contam. Hydrol. 45 (2000) 99–121.
[6] D. Morales, J.M. Gutiérrez, M.J. García-Celma, Y.C. Solans, A study of the relation between bicontinuous microemulsions and oil/water nano-emulsion formation, Langmuir 19 (2003) 7196–7200.
[7] I. Kayali, K. Qamhieh, U. Olsson, Formulating middle phase microemulsions using extended anionic surfactant combined with cationic hydrotrope, J. Disper. Sci. Technol. 32 (2011) 41–46.
[8] T.T. Phan, C. Attaphong, D.A. Sabatini, Effect of extended surfactant structure on interfacial tension and microemulsion formation with triglycerides, J. Am. Oil Chem. Soc. 88 (2011) 1223–1228.
[9] J.X. Zeng, J.J. Ge, G.C. Zhang, H.T. Liu, D.F. Wang, N. Zhao, Synthesis and evaluation of homogeneous sodium hexadecyl polyoxypropylene ether sulfates, J. Disper. Sci. Technol. 31 (2010) 307–313.
[10] W.X. Wang, J.B. Li, X.Y. Yang, P. Li, C.H. Guo, Q.H. Li, Synthesis and properties of a branched short-alkyl polyoxyethylene ether alcohol sulfate surfactant, J. Mol. Liq. 212 (2015) 597–604.
[11] S.J. Holder, B.C. Sriskantha, S.A. Bagshaw, I.J. Bruce, Headgroup effects on the krafft temperatures and self-assembly of x-hydroxyand x-carboxy hexadecyl quaternary

ammonium bromide bolaform amphiphiles: micelles versus molecular clusters? J. Colloid Interf. Sci. 367 (2012) 293–304.
[12] N. Ivanova, V. Starov, R. Rubio, H. Ritacco, N. Hilal, D. Johnson, Critical wetting concentrations of trisiloxane surfactants, Colloids Surf. A Physicochem. Eng. Asp. 354 (2010) 143–148.
[13] Q. Dai, J.S. Laskowski, The Krafft point of dodecylammonium chloride: pH effect, Langmuir 7 (1991) 1361–1364.
[14] T. Kaoru, M. Junryo, Krafft point depression of some zwitterionic surfactants by inorganic salts, J. Phys. Chem. 82 (1978) 1610–1614.
[15] Z.Q. Jin, Z.C. Xu, Q.T. Gong, S. Zhao, J.Y. Yu, Synthesis and properties of anionic surfactants containing oxyethylene group or/and branched tail, J. Disper. Sci. Technol. 32 (2011) 898–902.
[16] G.Y. Wang, W.S. Qu, Z.P. Du, Q.Y. Cao, Q.X. Li, Adsorption and aggregation behavior of tetrasiloxane-tailed surfactants containing oligo(ethylene oxide) methyl ether and a sugar moiety, J. Phys. Chem. B 115 (2011) 3811–3818.
[17] K.V. Roshchyna, S.V. Eltsov, A.N. Laguta, N.O. Mchedlov-Petrossyan, Micellar rate effects in the alkaline fading of crystal violet in the presence of various surfactants, J. Mol. Liq. 201 (2015) 77–82.
[18] D. Singharoy, S.S. Mati, S. Rakshit, S. Chall, S.C. Bhattacharya, Correlation of FRET efficiency with conformational changes of proteins in ionic and nonionic surfactant environment, J. Mol. Liq. 213 (2016) 33–40.
[19] M. Dahanayake, A.W. Cohen, M.J. Rosen, Relationship of structure to properties of surfactants. 13. Surface and thermodynamic properties of some oxyethylenated sulfates and sulfonates, J. Phys. Chem. 90 (1986) 2413–2418.
[20] B.W. Barry, R. Wilson, Micellar molecular weights and hydration of ethoxylated anionic and cationic surfactants, Colloid Polym. Sci. 256 (1978) 44–51.
[21] R. Varadaraj, J. Bock, P. Valint, S. Zushma, R. Thomas, Fundamental interfacial properties of alkyl-branched sulfate and ethoxy sulfate surfactants derived from Guerbet alcohols. 1. Surface and instantaneous interfacial tensions, J. Phys. Chem. 95 (1991) 1671–1676.
[22] G.Y. Wang, X. Li, Z.P. Du, E.Z. Li, P. Li, Butynediol-ethoxylate based trisiloxane: structural characterization and physico-chemical properties in water, J. Mol. Liq. 197 (2014) 197–203.
[23] T. Schuster, J.W. Krumpfer, S. Schellenberger, R. Friedrich, M. Klapper, K. Müllen, Effects of chemical structure on the dynamic and static surface tensions of short-chain, multi-arm nonionic fluorosurfactants, J. Colloid Interface Sci. 428 (2014) 276–285.
[24] D. Rauber, F. Heib, M. Schmitt, R. Hempelmann, Influence of perfluoroalkyl-chains on the surface properties of 1-methylimidazolium bis(trifluoromethanesulfonyl)imide ionic liquids, J. Mol. Liq. 216 (2016) 246–258.
[25] T. Tadros, Encyclopedia of Colloid and Interface Science, Springer, Wokingham, 2013 1242–1244.
[26] E. Ruckenstein, Effect of short-range interactions on spreading, J. Colloid Interface Sci. 179 (1996) 136–142.
[27] T.T. Zhao, H.J. Gong, G.Y. Xu, X.L. Cao, X.W. Song, H.Y. Wang, Investigation of salts tolerance of anionic surfactants in aqueous solutions, China Oilfield Chem 27 (2010) 112–118.
[28] E.H. Lucassen-Reynders, Anionic Surfactants: Physical Chemistry of Surfactant Action, Marcel Dekker Inc, New York, 1981 57–85.